Rock Mechanics and Rock Engineering (2023) 56:8305–8316
https://doi.org/10.1007/s00603-023-03485-y

ORIGINAL PAPER

Salt Creep: Transition Between the Low and High Stress Domains

Pierre Bérest[1] · Hakim Gharbi[1] · Laura Blanco-Martín[2] · Benoît Brouard[3] · Dieter Brückner[4] · Kerry L. DeVries[5] · Grégoire Hévin[6] · Gerd Hofer[7] · Christopher J. Spiers[8] · Janos L. Urai[9]

Received: 23 December 2022 / Accepted: 19 July 2023 / Published online: 16 August 2023

Abstract

In 2014–2016, creep tests were performed in a dead-end drift of the Altaussee mine, where temperature and relative humidity experience very small fluctuations. These tests, which were several months long, proved that the creep rate of a natural salt sample is much faster in the 0.2–1 MPa deviatoric stress range than the creep rate extrapolated from standard laboratory creep tests performed in the 5–20 MPa range. In addition, the quasi-steady strain rate is a linear function of stress, and it is faster when grain size is smaller. These findings were consistent with microphysical models of pressure solution creep (rather than dislocation creep, which is the governing creep mechanism at high stresses). A gap in experimental data remained in the 1–5 MPa range, calling for a follow-up experimental program. In 2016–2019, three multi-stage creep tests were performed on salt samples from Hauterives (France), Avery Island (Louisiana, USA), and Gorleben (Germany), which had been tested in the 0.2–1 MPa range during the 2014–2016 campaign. Loads of 1.5, 3, and 4.5 MPa were applied successively on each sample for 8 months. Steady state was not reached at the end of each 8-month stage. However, tests results suggest that, in the 0.2–3 MPa range, the relationship between the strain rate and the applied stress is linear, a characteristic feature of pressure solution. For these three samples, the relationship between strain rate and deviatoric stress departs from linearity when the deviator is larger than approximately 3–4.5 MPa, pointing to a transition to dislocation creep at higher deviatoric levels.

Highlights

- Very long duration uniaxial creep tests were performed under controlled conditions.
- The transient phase under low and moderate stress levels is long.
- Creep rate below 3 MPa is faster than extrapolated from high-stress creep tests.
- The strain rate-stress dependency is different at low and high deviatoric stresses.
- The transition between linear and non-linear dependency lies between 3–4.5 MPa.

Keywords Rock salt · Very long duration uniaxial creep tests · Slow creep rate · Strain rate–stress dependency · Transient creep at low stress

Pierre Bérest: Deceased July 28, 2022.

Janos L. Urai: Deceased May 28, 2023.

✉ Laura Blanco-Martín
laura.blanco_martin@minesparis.psl.eu

1 École Polytechnique, Palaiseau, France

2 Centre de Géosciences, Mines Paris, Université PSL, Fontainebleau, France

3 Brouard Consulting, Paris, France

4 Institut Für Gebirgsmechanik, Leipzig, Germany

5 RESPEC, Rapid City, SD, USA

6 Storengy, Bois-Colombes, France

7 Salinen Austria AG, Ebensee, Austria

8 Utrecht University, Utrecht, The Netherlands

9 GeoStructures Consultancy, Maastricht, The Netherlands

1 Introduction

Abundant literature has been dedicated to the mechanical behavior of salt. When a constant compressive deviatoric stress (σ) is applied to a salt sample at constant temperature and relative humidity, a fast transient shortening of the sample is observed first. After several weeks or months, the strain rate decreases significantly, though whether steady state is fully reached is still an open question. Experimental results on natural salt suggest that the quasi-steady strain rate is a non-linear function of the applied deviatoric stress, and independent of the mean stress. These results are consistent with microstructural considerations that suggest that the governing creep mechanism is dislocation motion inside the salt grains (Munson and Dawson 1984): steady state is reached when the formation rate of new dislocations equals the annihilation rate. However, these results were supported by tests performed in a relatively high deviatoric stress range ($\sigma \geq 5$ MPa, typically). The reason for this is that, in the small stress range, strain rates are exceedingly slow (lower than 10^{-11} s^{-1}, typically), and even small temperature changes can generate significant thermo-elastic strains, impeding any precise measurement of the viscoplastic strains generated by creep proper. The same can be said of relative humidity changes (Hunsche and Schulze 2002).

Based on theoretical arguments, geological evidence and creep tests performed on artificial salt samples, Spiers et al. (1990), Urai et al. (1986) and Urai and Spiers (2007) suggested that salt creep in the low deviatoric stress range is the result of pressure solution (provided intergranular brine is available and the grain size is small) rather than dislocation motion: at salt grain boundaries, mass transfer takes place from highly stressed zones (at the contact between grains) to less stressed zones through diffusion along intergranular brine films. Among other characteristic features, mentioned below, these works predicted that creep rates in the low-stress regime should be much faster than extrapolated from tests performed under high deviatoric stresses. Nevertheless, direct evidence from tests performed on natural rock salt under conditions typical of underground engineering activities was missing, motivating the research presented in this paper.

Since 1996, École Polytechnique and partners have conducted creep tests under small uniaxial stresses in dead-end drifts of the Varangéville mine (France) and the Altaussee mine (Austria). These tests, which were several months long to a few years long, took advantage of the very small fluctuations in temperature and relative humidity experienced in the drifts. More precisely, in 2014–2016 at the Altaussee mine, where the temperature is 7.8 °C and relative humidity is 68%, uniaxial creep tests ("Phase 1") were performed on natural salt samples from Avery Island (Louisiana, USA), Hauterives (France) and Gorleben (Germany) (Bérest et al. 2017). Samples were subjected to very small axial loads. Main results are presented in Table 1, together with the results of creep tests performed on other salt samples. This program, supported by the Solution Mining Research Institute (SMRI), proved the following:

- In the 0.2–1 MPa deviatoric stress range, the creep rate of a natural salt sample is much faster—by several orders of magnitude—than extrapolated from tests performed in the 5–20 MPa range;
- In this stress range, after several months, the quasi-steady strain rate is a linear function of the applied stress, at least approximately (though the transient phase is very long);
- The strain rate is faster when the grain size is smaller;
- Later tests (Bérest et al. 2019b) indicated that no creep is observed when the samples are set in dry, dessicant-buffered and hermetically sealed jackets.

These features were consistent with the work of Spiers et al. (1990), Urai et al. (1986) and Urai and Spiers (2007), and although not sufficient, they supported the pressure solution hypothesis. However, a gap in experimental data remained in the 1–5 MPa range, calling for a follow-up experimental program ("Phase 2"). Three of the existing creep devices were equipped with a force-multiplier—i.e., a cantilever system that allows application of higher stresses. To reduce the effects of specimen variability, three

Table 1 Strain rates at the end of each stage during $\sigma \leq 1$ MPa tests. The grain size was obtained at Utrecht University through the linear intercept method (Bérest et al. 2019a)

Salt	Load (MPa)	Duration (months)	Final creep rate ($\times 10^{-12}$/s)	Average grain size (mm)
Avery Island (AI#2)	0.20	19	1.1	8
Hauterives (HR#1)	0.20	11	0.3	10
Gorleben (GO#1)	0.20	11	3	3.8
Landes #2	0.22	12	2.5	5.5
Hauterives (HR#1)	0.40	9	0.8	10
Landes #1	0.60	12	9.0	5.5
Avery Island (AI#2)	0.60	8	4.8	8
Hauterives (HR#1)	0.60	8	1.2	10
Gorleben (GO#1)	1.07	8	12.5	3.8

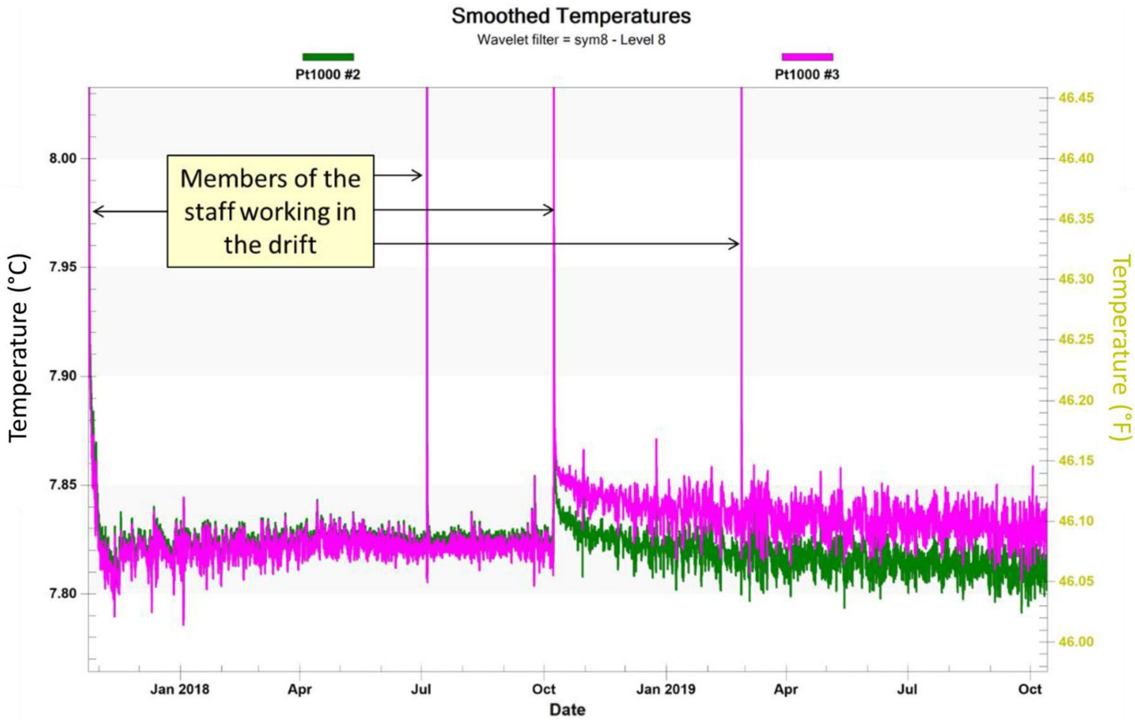

Fig. 1 Temperature in the drift from October 2017 to September 2019 (Phase 2)

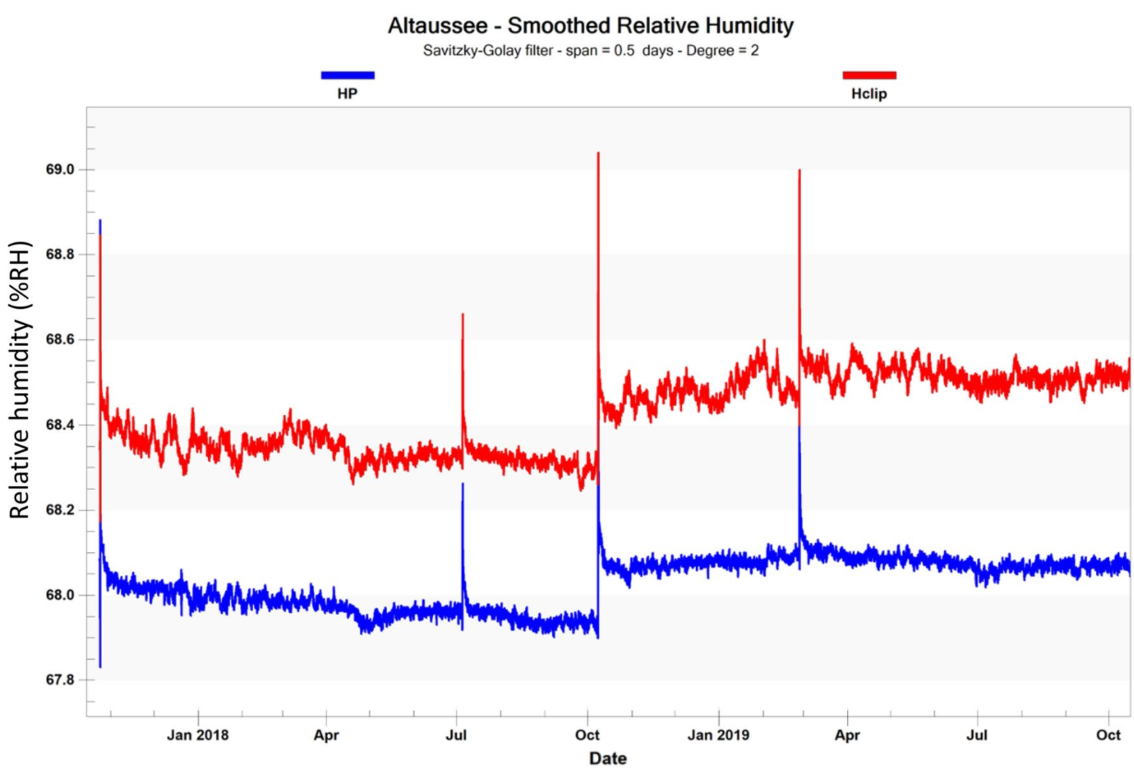

Fig. 2 Relative humidity in the drift from October 2017 to September 2019 (Phase 2)

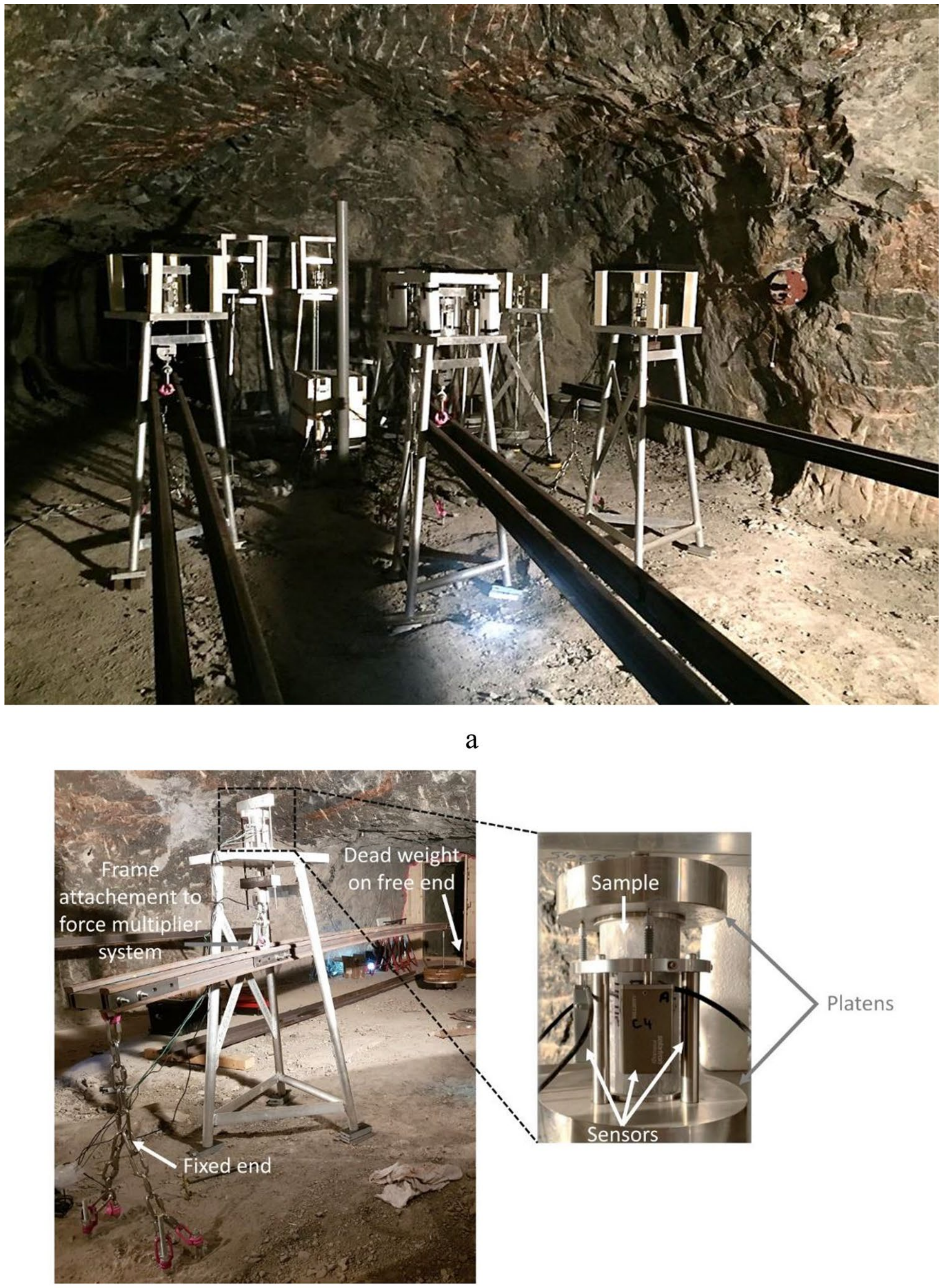

Fig. 3 The three cantilever systems used during the Phase 2 experiments reported here. **a** Overall view in the mine; **b** detail of a force-multiplier system and sample

salt samples used during the Phase 1 program (2014–2016, $\sigma \leq 1$ MPa range) were also used for the Phase 2 program (2016–2019, $\sigma > 1$ MPa range). Loads corresponding to axial stresses of $\sigma = 1.5$, 3, and 4.5 MPa (approximately) were applied successively on those samples over 8-month-long intervals to investigate the transition between low and moderate stress levels. The objective of this paper is to provide the results of these Phase 2 tests.

2 Testing Methodology

During creep tests of several months duration, uncertainties result mainly from fluctuations in temperature, humidity and applied stress, as well as from possible drift of the displacement sensors. The testing methodology is described in detail by Bérest et al. (2019a), to which the reader is invited to refer. Only its main features are recalled here.

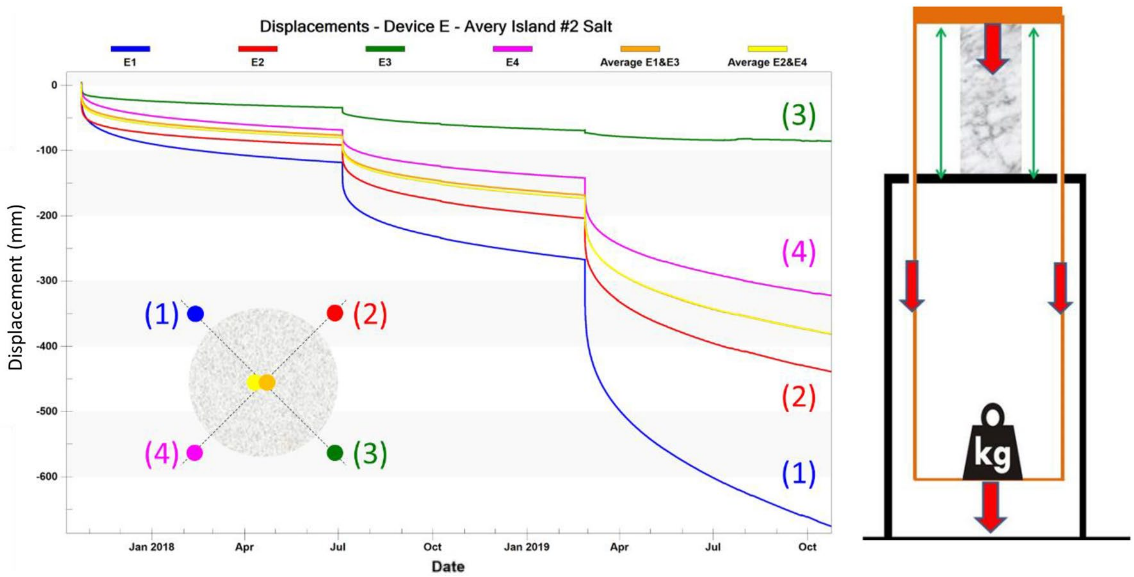

Fig. 4 A multi-stage creep test on the AI#2 sample during Phase 2 (Bérest et al. 2019b). Four displacement sensors, denoted E1–E4, are placed at angular intervals of 90° around the sample, as indicated in the lower left sketch (see also the thin arrows in the right-hand sketch), allowing for redundancy as well as control of drift and platen rotation. The applied stress is 1.59, 3.04, and 4.47 MPa, successively, and sample height is 140 mm

Table 2 Applied loads in MPa (Phase 2)

	Avery Island (AI#2)	Hauterives (HR#1)	Gorleben (GO#1)
1st Stage	1.59	1.83	1.63
2nd Stage	3.04	2.97	2.95
3rd Stage	4.47	4.52	4.58

2.1 Temperature and Humidity Fluctuations

When trying to assess small strain rates from laboratory tests, temperature and hygrometry fluctuations are a major concern. Both have a strong influence on creep rates. In addition, the linear thermal expansion coefficient of salt, which is in the order of $\alpha_{th} \approx 10^{-5}$ K^{-1}, is large: a change in sample temperature by $\delta T = 0.1°$ C during a 1-month period $\left(\delta t = 2.592 \times 10^6 \text{ s}\right)$ generates an *apparent* creep rate in the order of 10^{-12} s^{-1}—of the same order of magnitude as the typical creep rate to be measured.

Temperature is measured by two platinum sensors (Fig. 1, in which temperature evolution is smoothed using wavelets). The resolution of the temperature gauges is high (0.001 °C) but their accuracy is relatively poor. In fact, large temperature changes are observed in Fig. 1 in October 2017, July and October 2018, and March 2019, when members of the staff were working in the drift. The 8–10 October 2018 shift was longer than usual and was followed by a slow return of drift temperature to equilibrium. After several months, an offset is observed. Based on the results of earlier tests, this offset is believed to be due to the relatively poor accuracy of the sensors rather than an actual change of drift temperature (electrical offset after turning the sensors off and back on again). During quiescent periods, temperature fluctuations were typically ± 0.01 °C, yielding a strain fluctuation of approximately 0.1 μm/m.

Humidity changes were also measured, see Fig. 2. Two humidity sensors were used. Here again, large changes (more than 1%RH) are observed when members of the staff are working in the drift. During quiescent periods, fluctuations are ± 0.2%RH.

2.2 Applied Stress

During a creep test on a salt sample, fluctuations in the applied stress are also a concern. Small stress changes lead to recurring reductions of the observed creep rate even after the initial stress is restored (Gharbi et al. 2020; Wawersik and Preece 1984). For the Altaussee tests, dead weights were used and the applied force was perfectly constant. A cylindrical salt sample, whose diameter and height are $d = 70$ and $h = 140$ mm, respectively ($d = 65$ and $h = 130$ mm in the case of the two Landes samples), was set between two horizontal duralumin platens. During Phase 1, dead weights were set in the lower part of a mobile rigid frame. The frame weight was transmitted to the upper duralumin platen through a small metallic

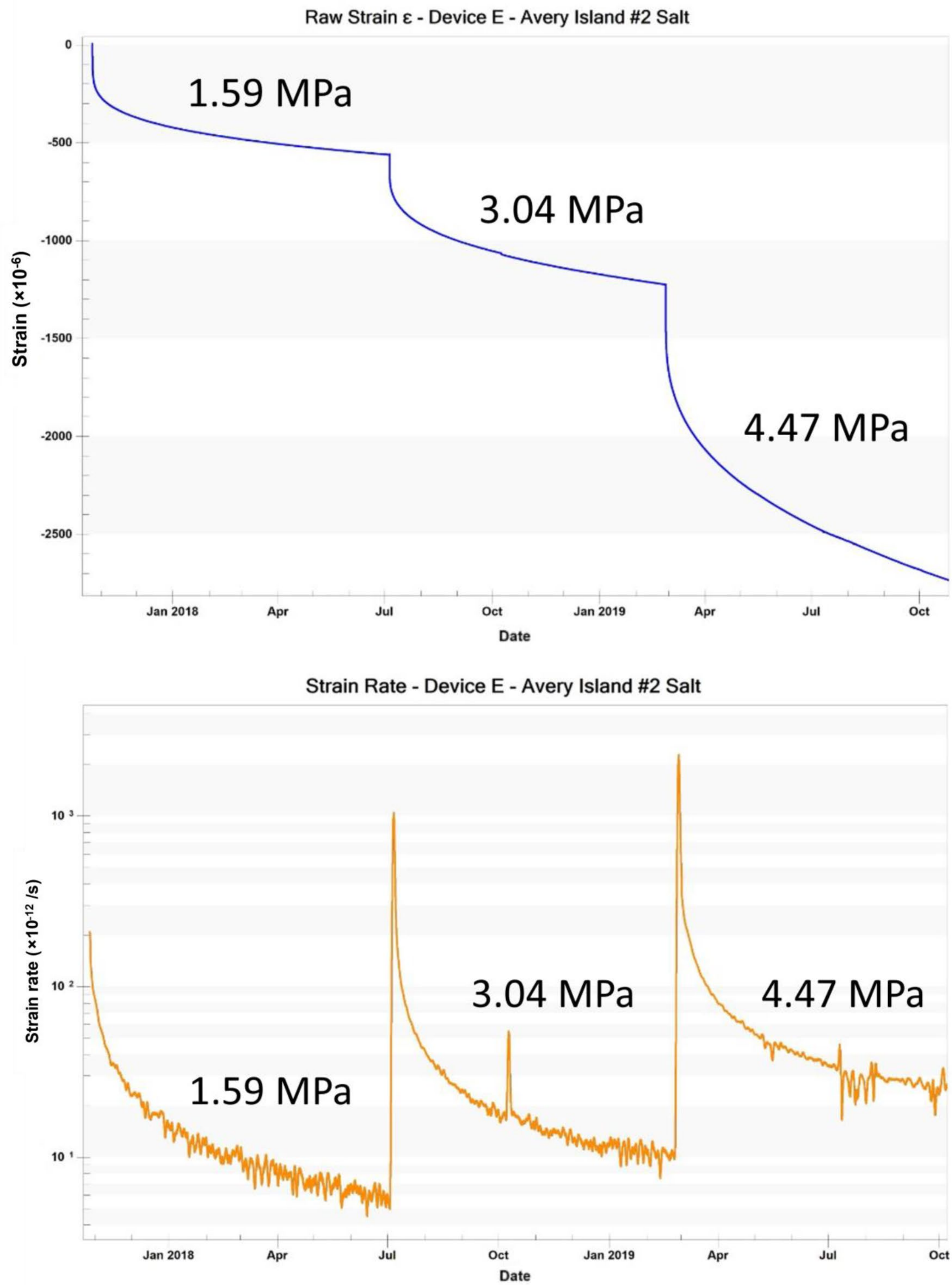

Fig. 5 Phase 2, AI#2 sample (strain and strain rate *vs.* time). Relative humidity and temperature are 68% and 7.8 °C, respectively

ball. The Phase 2 program called for the application of larger stresses. This system was not able to accommodate a large number of steel disks (the dead weight), and three creep devices were equipped with a force-multiplier—i.e., a cantilever system that provides sufficient force to achieve stresses up to 5 MPa on $d = 70$ mm samples. These devices

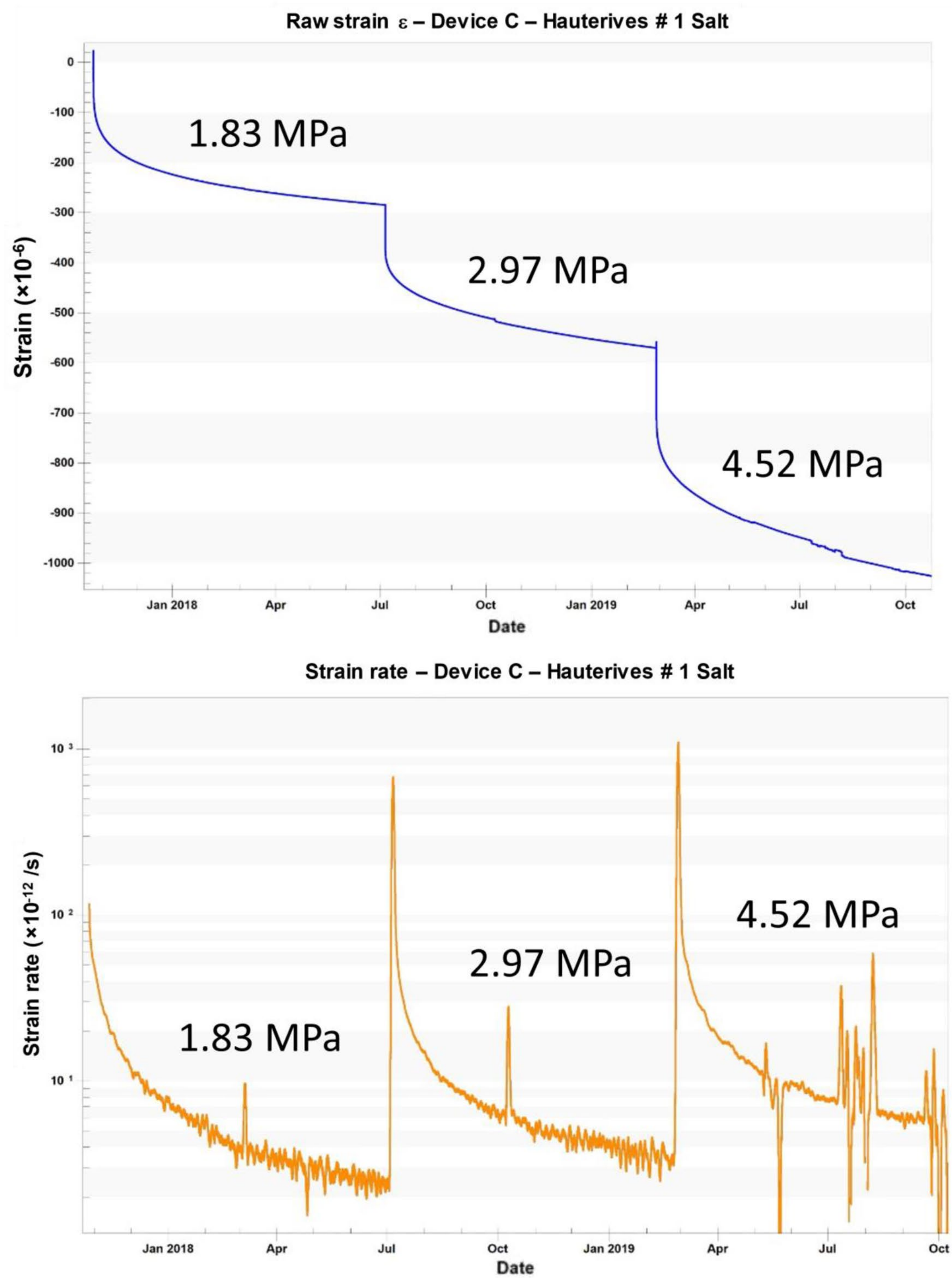

Fig. 6 Phase 2, HR#1 sample (strain and strain rate *vs.* time). Relative humidity and temperature are 68% and 7.8 °C, respectively

are shown in Fig. 3. It was checked that the additional weight added to the platen resulted in a force amplification factor of 5.27 when 25 kg disks were used and 5.43 when 10 kg disks were used.

2.3 Measurement of Axial Displacements

Creep rate can be computed by comparing strains $\varepsilon_1 = \delta h_1/h$ and $\varepsilon_2 = \delta h_2/h$ measured at two different

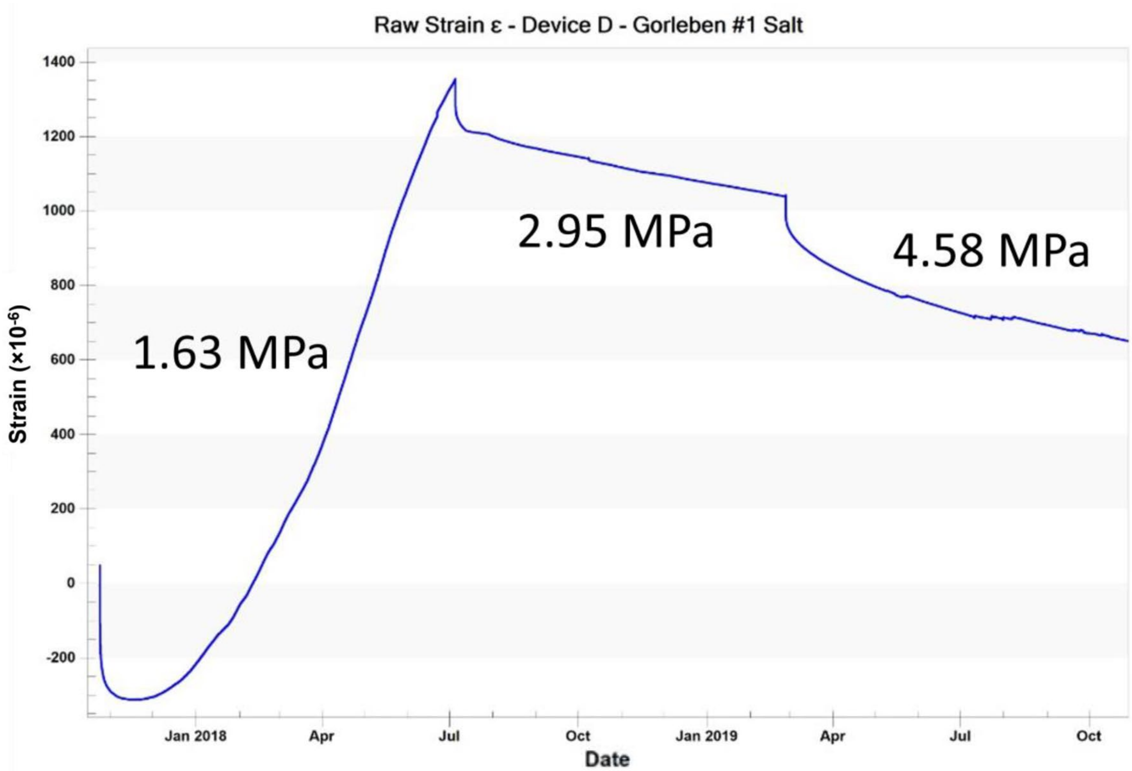

Fig. 7 Phase 2, GO#1 sample (strain *vs.* time). Relative humidity and temperature are 68% and 7.8 °C, respectively

times, t_1 and t_2, or $\dot{\varepsilon} = (\varepsilon_2 - \varepsilon_1)/(t_2 - t_1)$. For example, if $t_2 - t_1 = 10^5$ s (approximately one day) and $\dot{\varepsilon} = 10^{-12}\ \mathrm{s}^{-1}$ (lower bound as will be shown in the next section), then $\varepsilon_2 - \varepsilon_1 = 10^{-7}$. Therefore, a reasonable assessment of weekly strain rates demands that strain be measured with an accuracy of 10^{-7}. The heights of most samples tested in this study were $h = 140$ mm; therefore, axial displacements must be measured with an accuracy of approximately 10^{-8} m. Special sensors (Solartron linear encoders) were used; their resolution is 1/80 µm ($1.25 \cdot 10^{-8}$ m).

To provide some redundancy and monitor for drift of the displacement sensors, four high-resolution displacement sensors were positioned in two vertical planes at a 90° angle (see the horizontal cross-section in the lower left part of Fig. 4). The four displacements shown in Fig. 4 are not equal, suggesting sensor drift and/or relative rotation of the stiff duralumin upper platen. The average displacements of the two pairs of diametrically opposed sensors (1 and 3, and 2 and 4, respectively) should be equal if no drift occurs. In fact, they exactly overlap (see Fig. 4). This strongly suggests that there is no, or exceedingly small, drift of the sensors and that, in addition to the average vertical displacement of the upper duralumin platen, a rotation of this platen takes place. In fact, the rotation stabilizes after several months, and the cumulated rotation of the vertical axis of the upper platen is $5 \cdot 10^{-4}$ rad, too small of a value to significantly modify the stress distribution applied by the upper platen on the sample. This rotation may be due to the initial crushing or flattening of small irregularities with a typical height of 10 µm that are randomly distributed across the upper and lower faces of a sample (Bérest et al. 2019a).

2.4 Computation of Strain Rates

Strains are recorded every minute; in principle, strain rates could be computed every minute. However, the computed rates determined at this frequency experience erratic variations because of incessant changes in thermo-elastic strains—temperature changes seem to be correlated with atmospheric pressure fluctuations, but they are smaller than what is predicted by the adiabatic assumption ($\dot{T}/T = (1 - 1/\gamma)\dot{P}/P$), suggesting that heat transfer from the drift air to the rock mass is fast. In principle, sample height changes could be corrected from room-temperature fluctuations. In reality, propagation of temperature changes in the sample through conduction is a relatively slow process (typically, 1 h), and separation of thermo-elastic strains from viscoplastic strains within the sample proves difficult. For this reason, the strain rates are averaged through a least-square method over a time span significantly greater than the

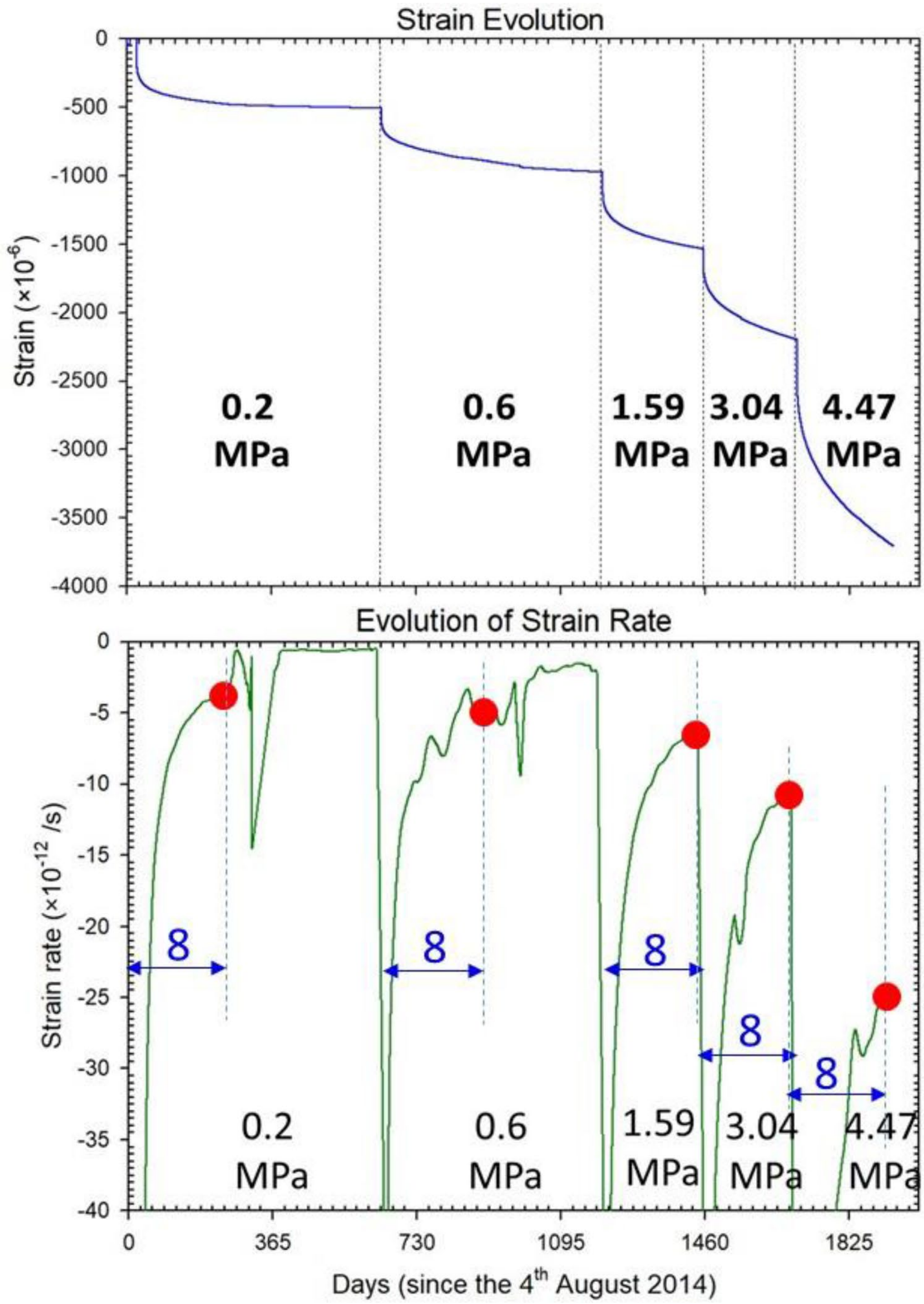

Fig. 8 Phases 1 and 2, AI#2 sample (strain and strain rate *vs.* time). Relative humidity and temperature are 68% and 7.8 °C, respectively (compression is negative in this figure). Dots: strain rate after 8 months

acquisition frequency; this way, the thermo-elastic influence due to the (very small) temperature fluctuations is attenuated. A 7-day average span was selected.

2.5 A Comment on Steady State

Determining whether steady state has been reached is an important objective of a creep test. From a scientific perspective, it is a difficult task, and some subjectivity is necessarily involved. A visual inspection of the strain *vs.* time curve cannot provide a sufficiently precise answer, and strain rate evolution must be computed. The strain rate may appear constant during, say, one month; however, it is impossible to be certain that the strain rate would have remained constant if the test had lasted one year longer (a positive monotonously decreasing function of time may or may not

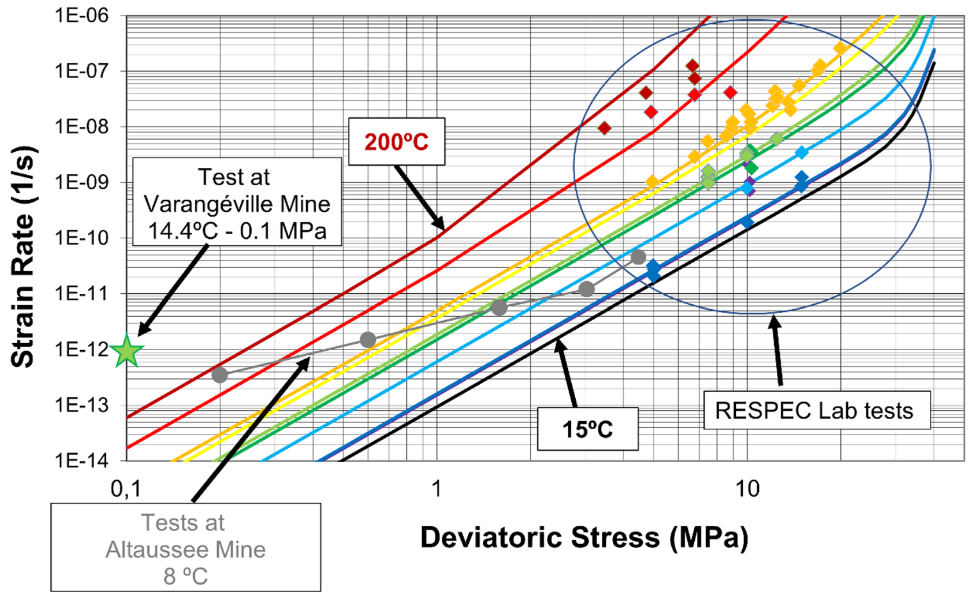

Fig. 9 Tests conducted on Avery Island samples at the RESPEC laboratory (at high σ and T, colored dots) and in the Altaussee mine (at small σ and 7.8 °C, black dots). The colored lines correspond to fitting of the RESPEC tests with the Munson–Dawson model (Munson and Dawson 1984)

have a zero asymptotic value). To allow simple comparisons, all creep stages during Phase 2 lasted 8 months (from Table 1, the durations of the creep stages during Phase 1 are not the same). In most cases, as it will be shown below, it is clear that steady state was not reached after such a duration. However, this is not a problem for the purpose sought here, which is to investigate the relationship between the creep rate and the deviatoric stress (we assume linear elasticity and viscoplasticity); in fact, for a proper analysis, the effect of the deviatoric stress must be separated from that of time.

3 Main Results

The Phase 2 testing campaign began on October 20, 2017 and ended on October 28, 2019. The stress conditions applied are listed in Table 2. Note that because the deadweight disks are not perfectly identical, it was not possible to apply the exact same load to each specimen.

The creep test results are presented in Figs. 5, 6, 7 for AI#2, HR#1 and GO#1 samples, respectively. The strain *vs.* time curves are somewhat "bumpy" in late July 2019 and early August 2019 (instantaneous offsets in the strain values). This phenomenon is also observed for other tests during the same period and is not correlated to significant changes in temperature, humidity or atmospheric pressure. Overall, displacements during the two-year tests are 0.14 mm (10^{-3} strain) for HR#1 and 0.36 mm ($2.6{\cdot}10^{-3}$ strain) for AI#2, confirming that Avery Island salt is more creep-prone than Hauterives salt. It should be noted that the behavior of the GO#1 sample is whimsical starting during Phase 1, see Bérest et al. (2019a): "swelling" over long periods (0.2 mm during the 1.63 MPa step, a $1.4{\cdot}10^{-3}$ strain) partially or completely obscures creep of the sample. The origin of this phenomenon is not perfectly understood, and strain rates were not computed for this sample.

As the figures show, steady state had not been reached by any of the samples at the end of each 8-month-long stage. This was also observed during some of the Phase 1 stages, which comprised longer creep stages (Bérest et al. 2019a). It is difficult to assess whether the transient period must be interpreted as transient creep proper, or as crushing or flattening of irregularities of the upper and lower surfaces of the sample, or both. For this reason, when a strain rate is specified, duration of the step should be provided. Figure 8 shows all stages conducted on sample AI#2, both during Phase 1 and Phase 2 (note that compression is negative in this plot).

In Fig. 9, the strain rates at the end of the five stages (black dots) of the AI#2 Altaussee test are compared to a data base provided by RESPEC (DeVries 1988), which includes tests performed under high stresses and temperatures (σ> 3.5 MPa). Note that sample preconditioning, as well as the tests duration and conditions are not the same for all samples, so the analysis can only be qualitative (it is also necessary to separate the effect of time from that of the stress deviator and the temperature). A first examination suggests that in the σ < 3 MPa stress range, the strain rate is proportional to the applied stress—at least approximately. Moreover, the behavior of the salt samples experiences a significant change when the applied stress is in the 3–4.5 MPa range. In fact, the transition between the "low-stress" behavior (governed in theory by pressure solution creep) and the "high-stress" behavior (governed in theory by dislocation creep) seems to lie between 3–4.5 MPa.

4 Conclusions and Perspectives

A 5-year creep test campaign was performed on three salt samples from Avery Island (Louisiana), Gorleben (Germany), and Hauterives (France). During Phase 1 (Bérest et al. 2017; Bérest et al. 2019a), several stresses belonging to the 0.2–1 MPa range were applied, and the results (that quasi-steady strain rate is a linear function of the deviatoric stress) are consistent with creep being governed by pressure solution. During Phase 2, three stress stages (1.5, 3 and 4.5 MPa) were applied successively on each sample. The duration of each stress stage was 8 months. Similar to Phase 1, steady state was not reached at the end of each loading stage. A change in the response could be observed, suggesting that the transition between the “low-stress” behavior (governed in theory by pressure solution creep) and the “high-stress” behavior (governed in theory by dislocation creep) lies between 3–4.5 MPa. The notion of different governing creep mechanisms under different thermomechanical conditions is of substantial significance for engineering applications as it helps improve predictions of underground structures, such as storage caverns or nuclear waste repositories. Indeed, most of the time, and in most of the salt formation, deviatoric stresses are small and predictions based on a constitutive model that considers this notion can be significantly different from those based on standard laws (see, for instance, Tijani et al. 2009; Bérest et al. 2009; Marketos et al. 2016; van Sambeek and DiRienzo 2016; Cornet et al. 2018; Sobolik and Ross 2022; Hunfeld et al. 2022).

The tests were performed in uniaxial, drained conditions. Future testing is being planned with jacketed specimens tested in conventional triaxial cells, i.e., under confining pressure P (with P equal to two principal stresses) to more closely replicate in situ conditions. Additionally, microscopic investigations to characterize the salt microstructure and brine content at the grain and grain boundary scales would help identify the dominant creep mechanisms operating at low and high stress conditions in tests on natural salts. For such purposes, microanalysis should be conducted on both deformed and non-deformed material, and ideally also on dried and undried samples. Finally, the tests should be interpreted through modeling to separate the effect of time (steady state is not fully reached) from that of the stress deviator and the temperature, and also to account for the loading history of the samples.

Acknowledgements Unfortunately, Professor Pierre Bérest passed away on July 28, 2022, and Professor Janos Urai passed away on May 28, 2023. We are grateful for their important contributions to the topic discussed in this paper. This project was supported by the Solution Mining Research Institute (SMRI). The authors are grateful to Steve Bauer (SMRI sponsor) and to the members of the SMRI Research Committee for their helpful comments. Special thanks to Kathy Sikora.

Author Contributions All authors contributed to the study. Conceptualization: PB, CJS, JLU; Methodology: PB, BB, HG; Experiments and samples: PB, HG, BB, LBM, DB, KLDV, GH, GH. Funding acquisition and supervision: PB.

Funding This study was funded by Solution Mining Research Institute.

Data availability Not applicable (the data are shown in graphical form).

References

Bérest P, Brouard B, Karimi-Jafari M (2009) The effect of small deviatoric stresses on cavern creep behavior. In: 9th Int. Symp. Salt, Beijing, China, pp 574–589

Bérest P, Gharbi H, Brouard B, Hofer G, Stimmisher S, Brückner D, DeVries KL, Hévin G, Spiers CJ, Urai JL, Bauer S (2017) Very slow creep tests as a basis for cavern stability analysis, SMRI Research Report RR2017–1

Bérest P, Brouard B, Brückner D, DeVries KL, Gharbi H, Hévin G, Hofer G, Spiers CJ, Urai JL (2019a) Very slow creep tests on salt samples. Rock Mech Rock Eng. https://doi.org/10.1007/s00603-019-01778-9

Bérest P, Brouard B, Brückner D, DeVries KL, Gharbi H, Hévin G, Hofer G, Spiers C, Urai JL, Bauer S (2019b) Very slow creep tests as a basis for cavern stability analysis, Phase 2, SMRI Research Report RR2020–1 (U2017–2)

Cornet JS, Dabrowski M, Schmid DW (2018) Long-term creep closure of salt cavities. Int J Rock Mech Min Sci. https://doi.org/10.1016/j.ijrmms.2018.01.25

DeVries KL (1988) Viscoplastic laws for Avery Island salt. RE/SPEC Inc., Rapid City, SD, RSI-0333, Prepared for Stone & Webster Engineering Corporation, Boston

Gharbi H, Bérest P, Blanco-Martín L, Brouard B (2020) Determining upper and lower bounds for steady state strain rate during a creep test on a salt sample. Int J Rock Mech Min Sci. https://doi.org/10.1016/j.ijrmms.2020.104452

Hunfeld LB, Breunese J, Wassing B (2022) The influence of a threshold stress for pressure solution creep on cavern convergence and subsidence behavior—a FEM study. In: Proc. 10th Conf. Mech. Beh. Salt, Utrecht University, The Netherlands, pp 577–589

Hunsche U, Schulze O (2002) Humidity induced creep and its relation to the dilatancy boundary. In: Proc. 5th Conf. Mech. Beh. Salt, Bucharest, Romania, pp 73–87

Marketos G, Spiers CJ, Govers R (2016) Impact of rock salt creep law choice on subsidence calculations for hydrocarbon reservoirs overlain by evaporite caprocks. J Geo Res Solid Earth 121:4249–4267. https://doi.org/10.1002/2016JB012892

Munson DE, Dawson PR (1984) Salt constitutive modeling using mechanism maps. In: Proc. 1st Conf. Mech. Beh. Salt, University Park, PA, pp 717–737

Spiers CJ, Schutjens PMTM, Brzesowsky RH, Peach CJ, Zwart LJL (1990) Experimental determination of the constitutive parameters governing creep of rocksalt by pressure solution. Geol Soc Lond Engl 54:215–227. https://doi.org/10.1144/GSL.SP.1990.054.01.21

Sobolik SR, Ross TSA (2022) Geomechanical analysis of oil storage caverns in salt domes with a low stress creep mechanism added to the M-D model. In: Proc. 10th Conf. Mech. Beh. Salt, Utrecht University, The Netherlands, pp 662–673

Tijani M, Hadj-Hassen F, Gatelier N (2009) Improvement of Lemaitre’s creep law to assess the salt mechanical behavior for a large range of the deviatoric stress. In: 9th Int. Symp. Salt, Beijing, China, pp 135–147

Urai JL, Spiers CJ, Zwart HJ, Lister GS (1986) Weakening of rock salt by water during long-term creep. Nature 324(6097):554–557 van Sambeek LL, DiRienzo AL (2016) Analytical solutions for stress distributions and creep closure around open holes or caverns using multilinear segmented creep laws. In: Proc. SMRI Fall Meeting, Salzburg, Austria

Wawersik WR, Preece DS (1984) Creep testing of salt: procedures, problems and suggestions. In: Proc. 1st Conf. Mech. Beh. Salt, University Park, PA, pp 421–449